

Supporting Information

Redox Sensitive Self-Assembling Dipeptide for Sustained Intracellular Drug Delivery

Sameer Dhawan,^a Sukanya Ghosh,^b R. Ravinder,^c Sachendra S. Bais,^d Soumen Basak,^d N. M. Anoop Krishnan,^{c,e} Manish Agarwal,^f Manidipa Banerjee^b and V. Haridas*^a*

^aDepartment of Chemistry, Indian Institute of Technology Delhi, New Delhi, India.

^bKusuma School of Biological Sciences, Indian Institute of Technology Delhi, New Delhi, India.

^cDepartment of Civil Engineering, Indian Institute of Technology Delhi, New Delhi, India.

^dNational Institute of Immunology, Aruna Asaf Ali Marg, New Delhi, India.

^eDepartment of Material Science & Engineering, Indian Institute of Technology Delhi, New Delhi, India.

^fComputer Service Center, Indian Institute of Technology Delhi, New Delhi, India.

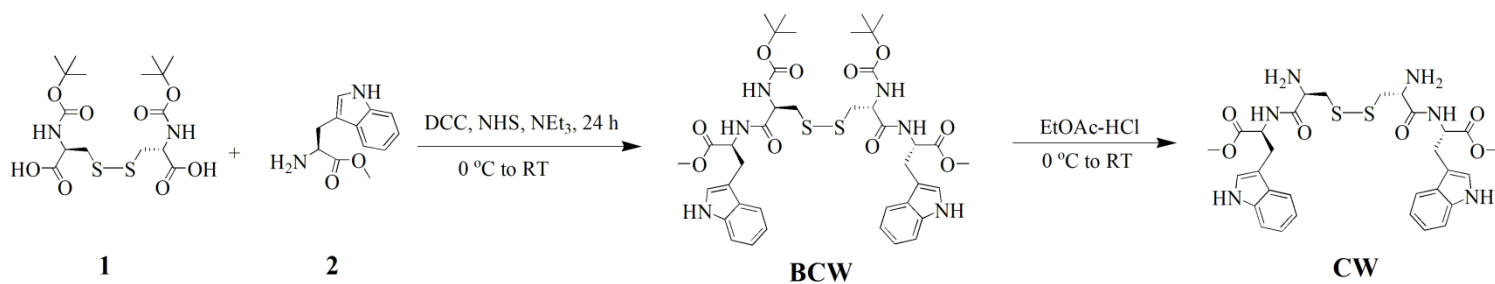
* Corresponding authors:

E-mail: haridasv@chemistry.iitd.ac.in

Tel.: +91-11-2659 1380

E-mail: mbanarjee@bioschool.iitd.ac.in

Tel.: +91-11-2659 7538



Scheme S1: Synthesis of dipeptide **BCW** and corresponding *N*-deprotected derivative **CW**.

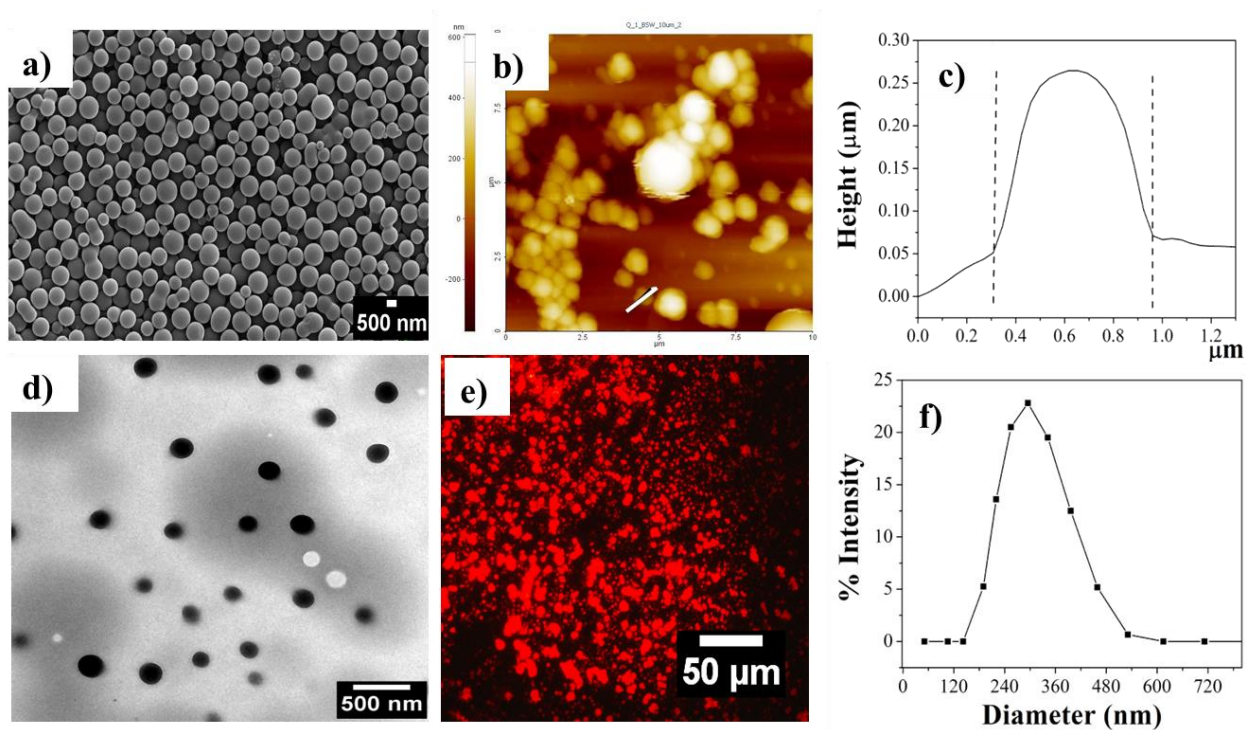


Figure S1: Microscopic and size distribution analyses of **BCW**. Compound **BCW** in MeOH (1 mg/ml) a) SEM, b) AFM, c) AFM cross-sectional analysis along the line, d) TEM, e) fluorescence microscopic images of **BCW**+0.02 equivalents of Rhodamine B ($\lambda_{\text{ex}} = 510\text{-}560$ nm), f) DLS of **BCW**.

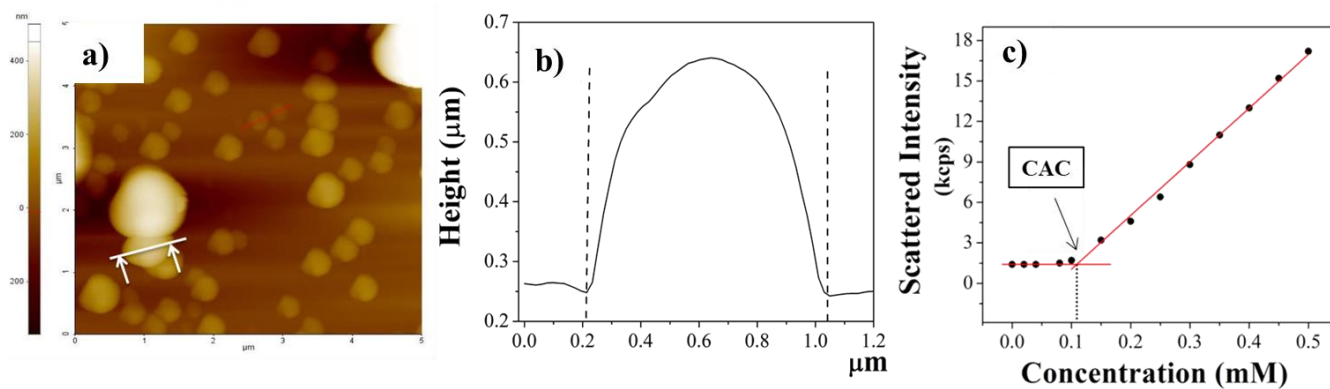


Figure S2: Morphological analysis of **CW** dissolved in water (1 mg/ml) a) AFM, b) AFM cross-sectional analysis along the line; c) Scattered intensities collected from the different concentration solutions of **CW** in water. The intersection point in the plot corresponds to CAC.

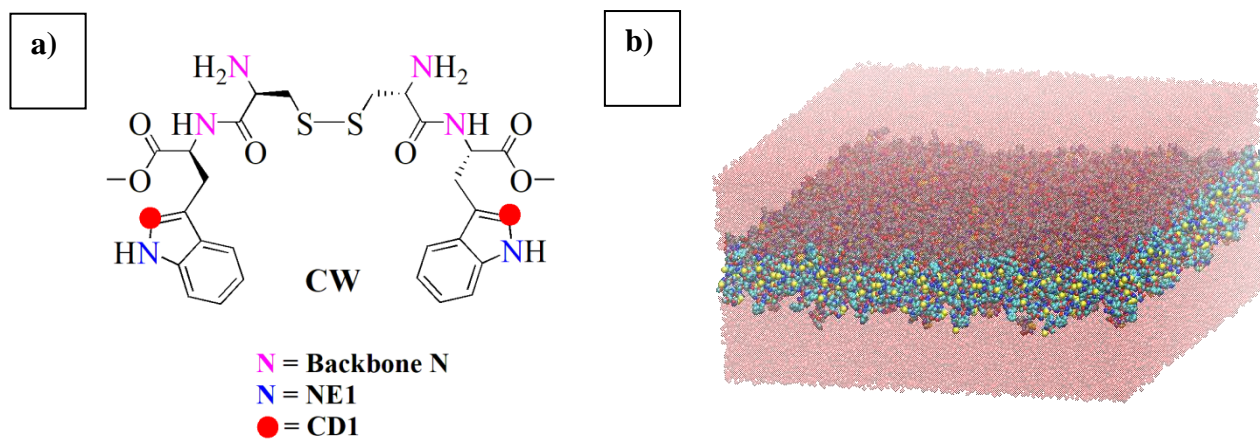


Figure S3: a) An initial labeled structure of **CW**, b) A snapshot of initial system configuration of flat dipeptide membrane.

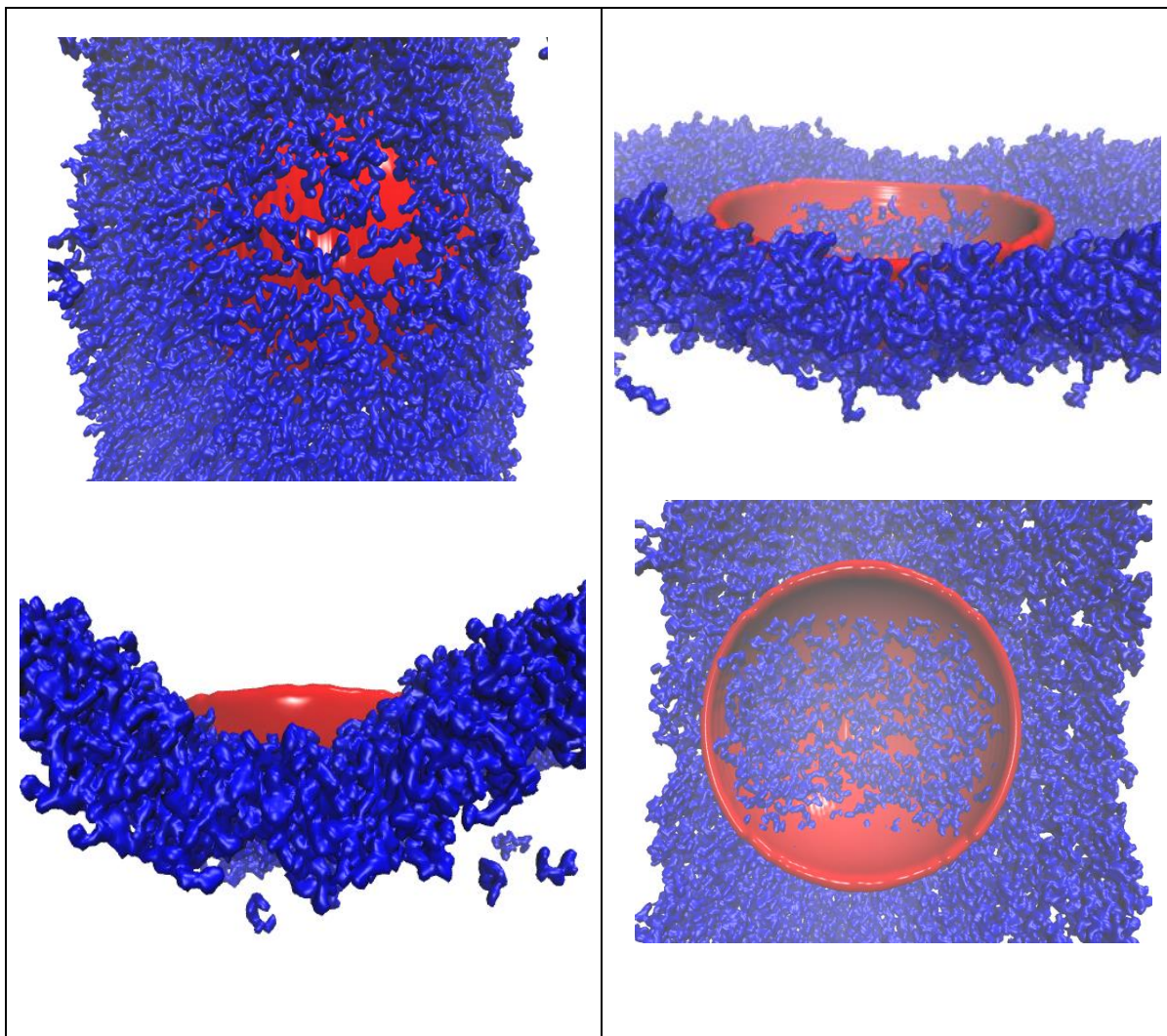


Figure S4: Snapshots of dipeptide membrane (blue) with a spherical fit (red).

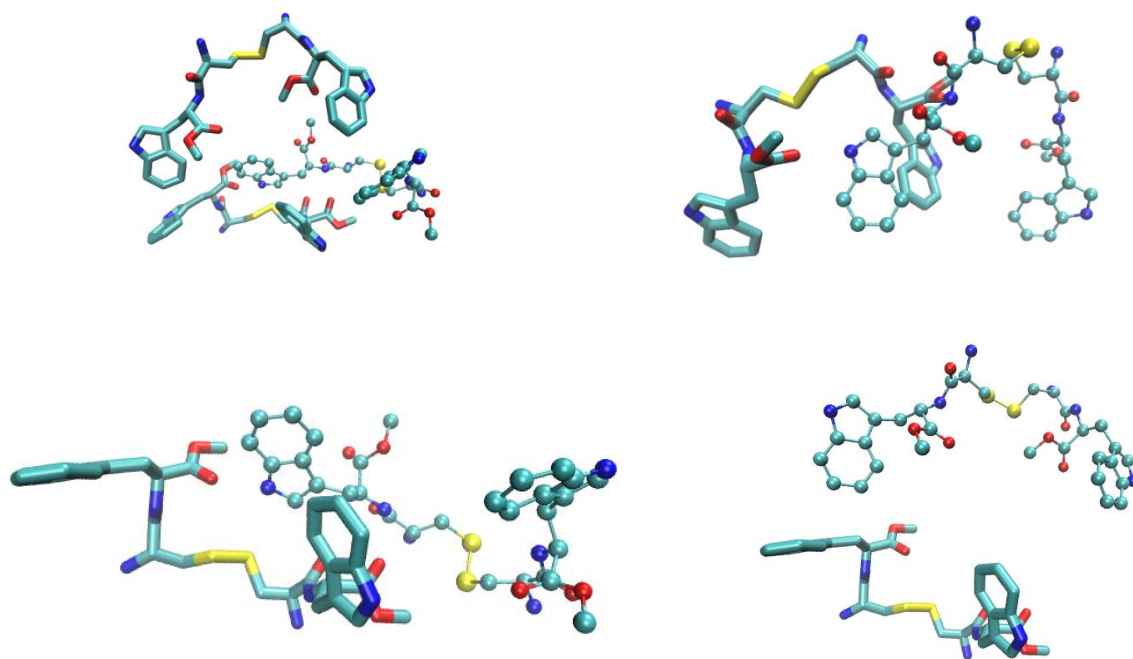


Figure S5: Different snapshots of the arrangement of two **CW** molecules exhibiting preferential attraction of the tryptophan groups.

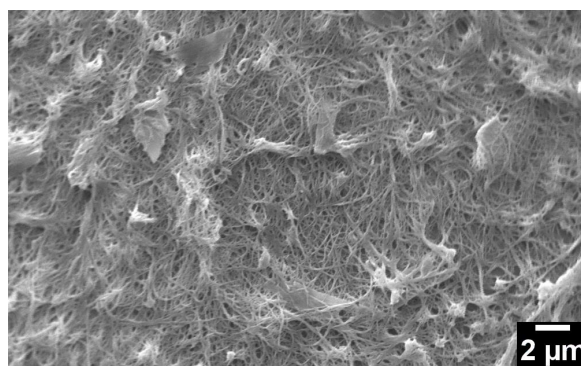
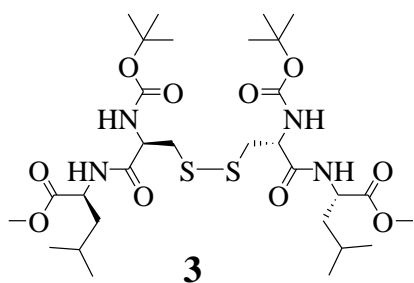


Figure S6: Chemical structure of leucine analogous of **BCW** and its fibrous self-assembly.

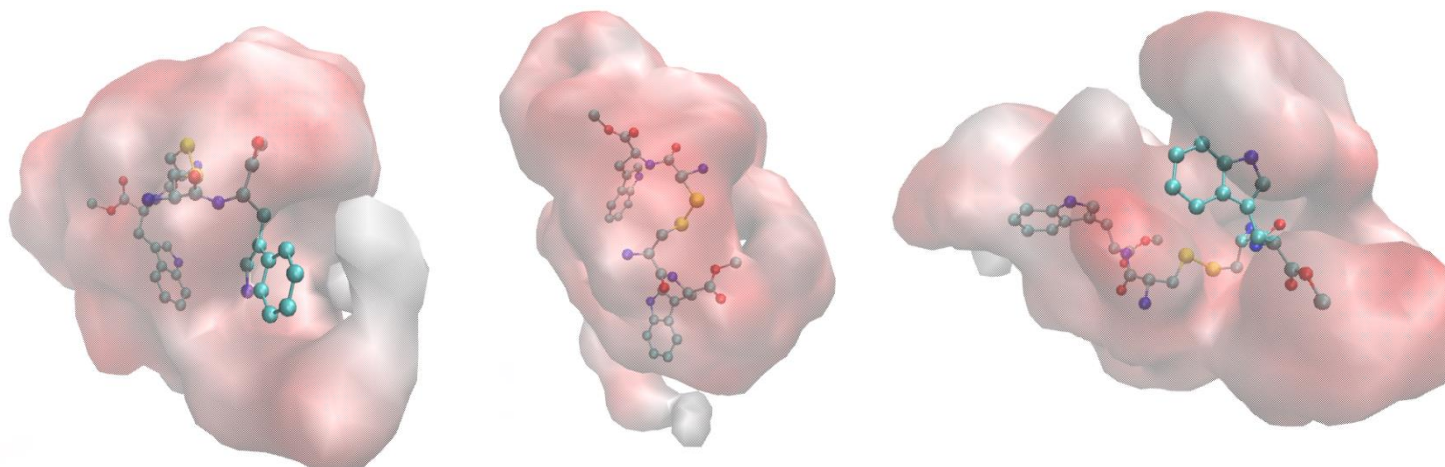


Figure S7: Snapshots of different orientation of **CW** molecule in water, showing the preferential attraction of water cloud (gradient shown from white to red) towards backbone than tryptophan residues. A cavity of water can be seen clearly around tryptophan.

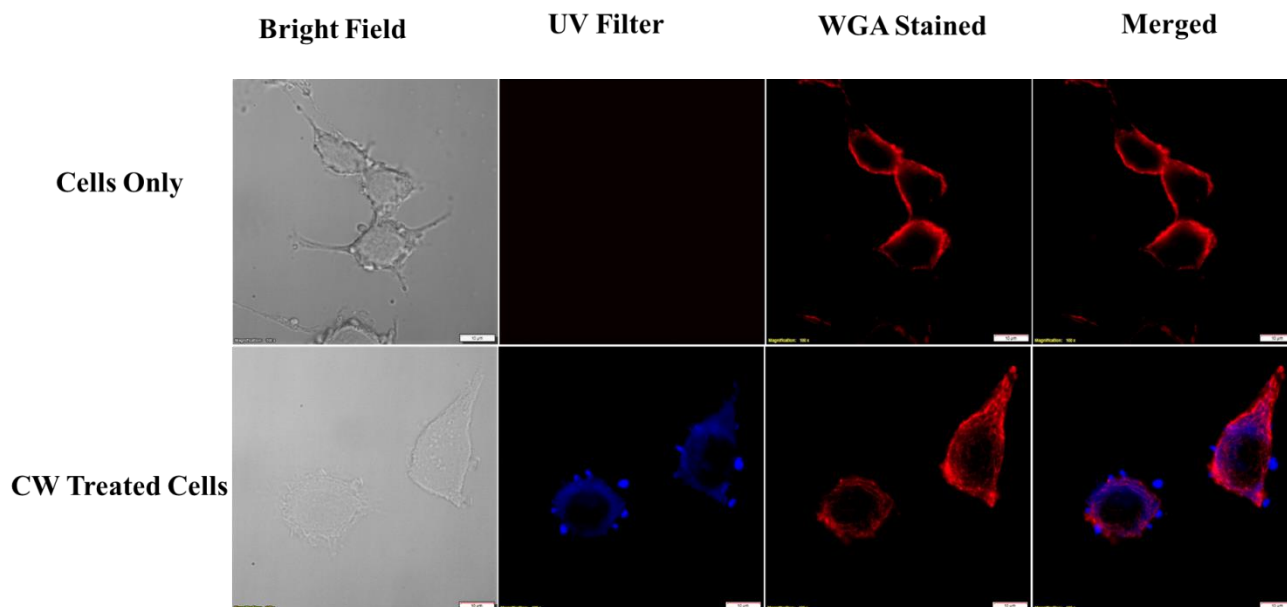


Figure S8: Cellular internalization of **CW** vesicles by CLSM in MDA-MB-231 cells. All images were captured at 100x magnification

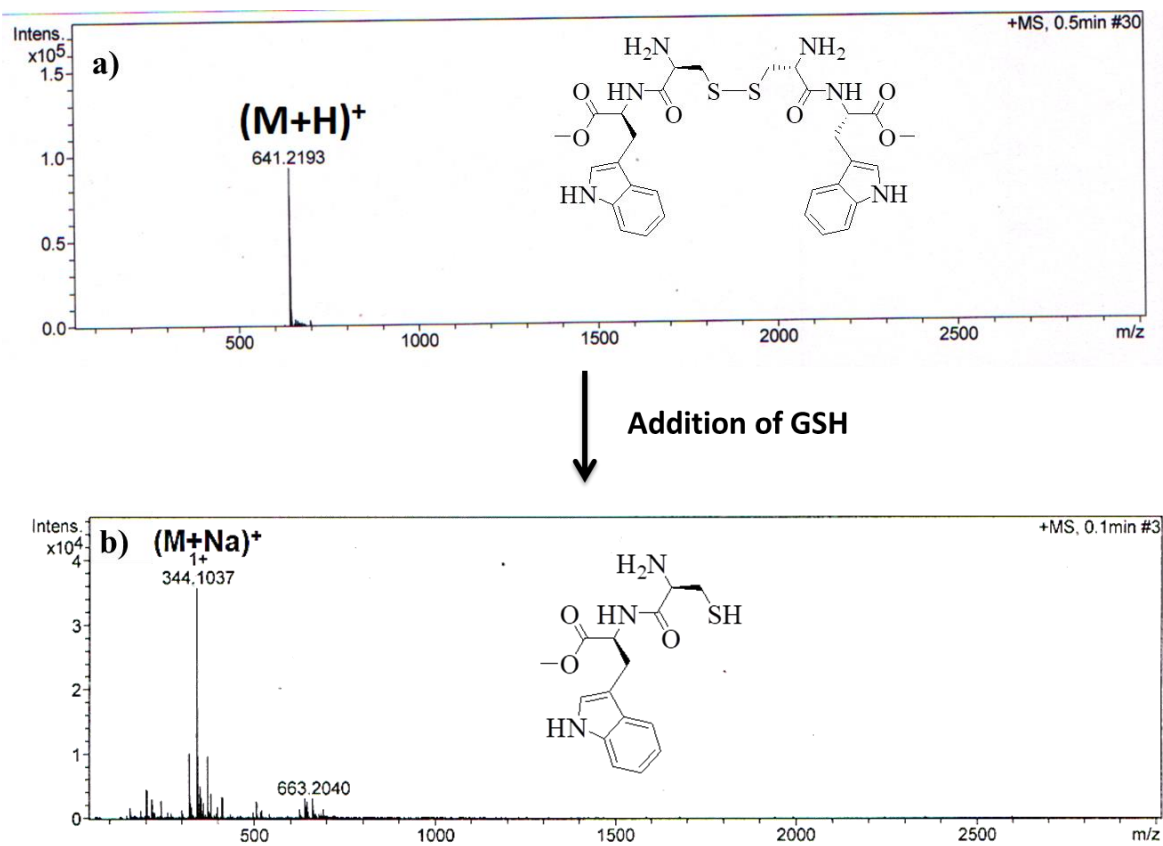


Figure S9: ESI-MS spectra of **CW** before and after the addition of GSH.

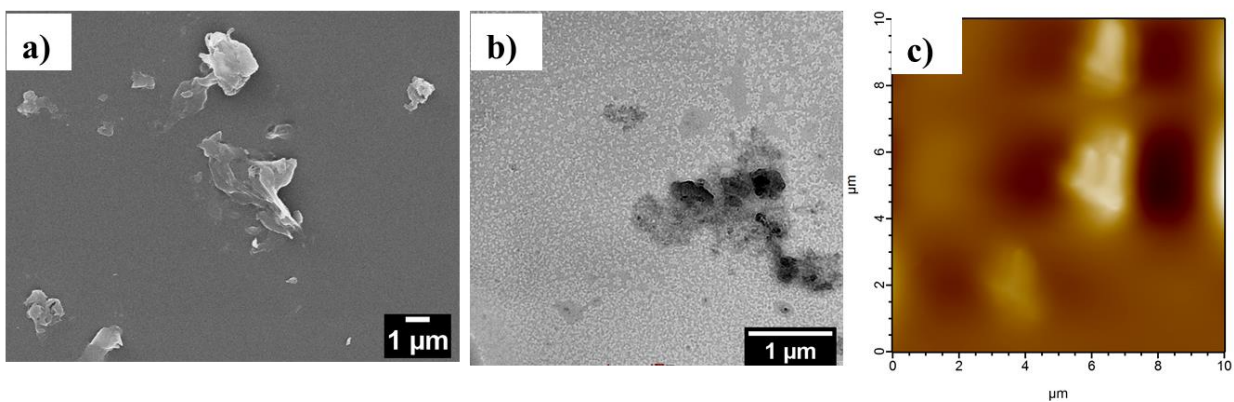


Figure S10: Morphological analysis of **CW** vesicles after the addition of GSH (10 mM) a) SEM, b) TEM, c) AFM.

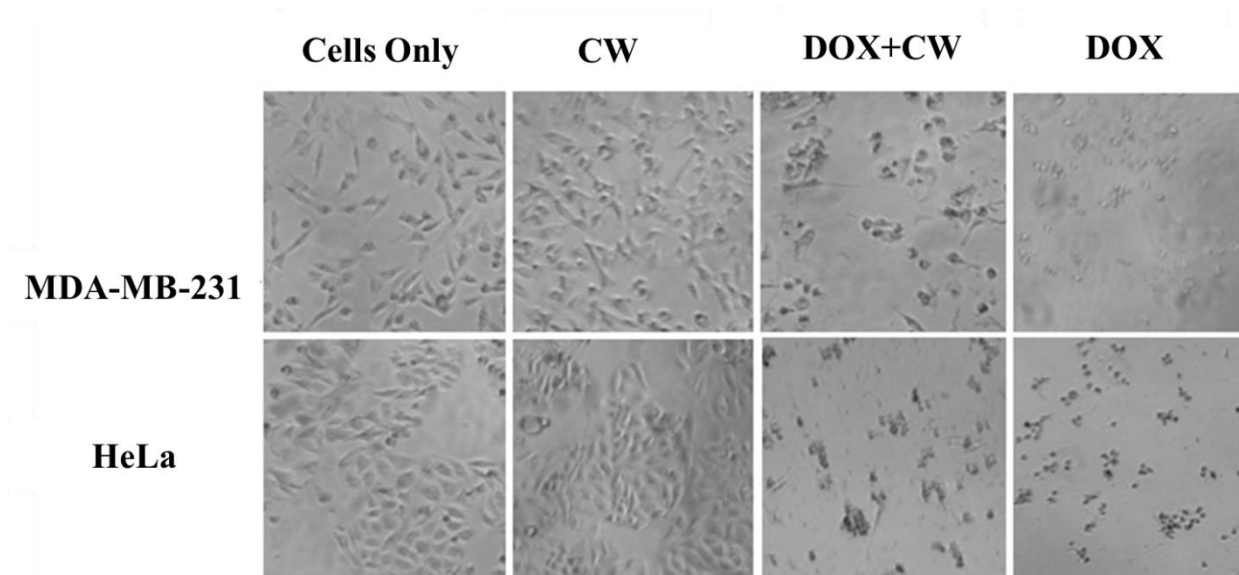


Figure S11: Optical microscopic images of treated cells after 72 h.

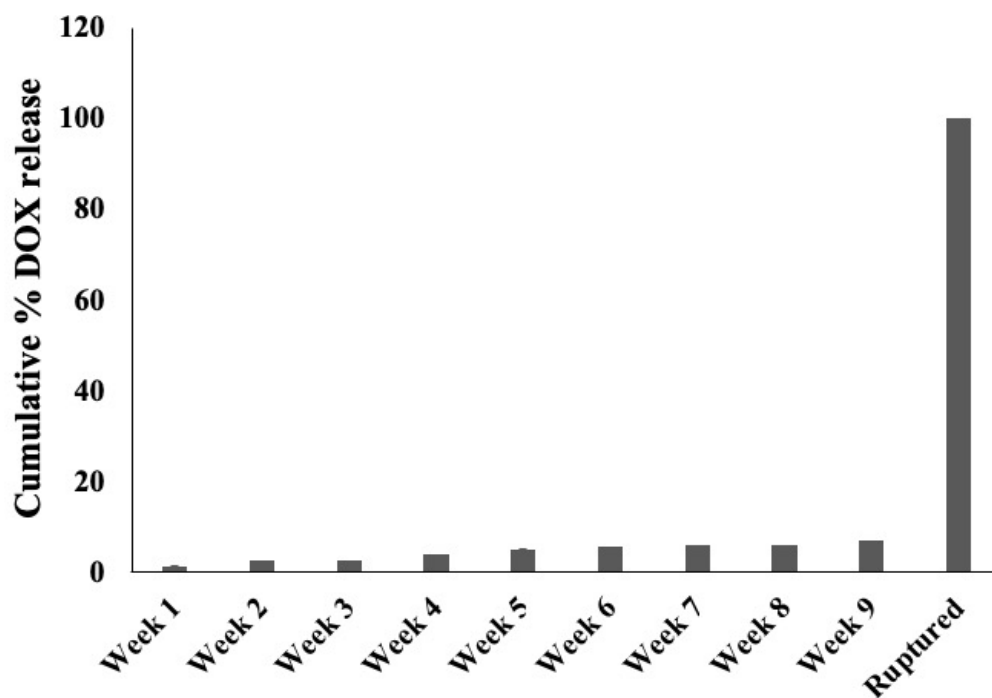


Figure S12: *In vitro* stability study of DOX-loaded CW vesicles stored in the dark at 4 °C.

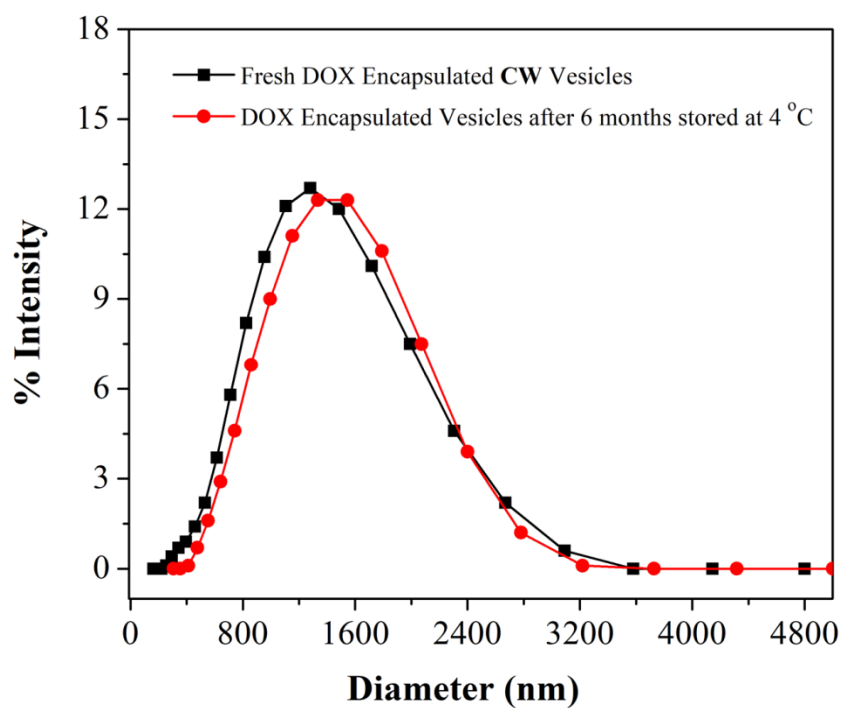


Figure S13: Aggregation study of DOX loaded CW vesicles stored in the dark at 4 °C using DLS data.

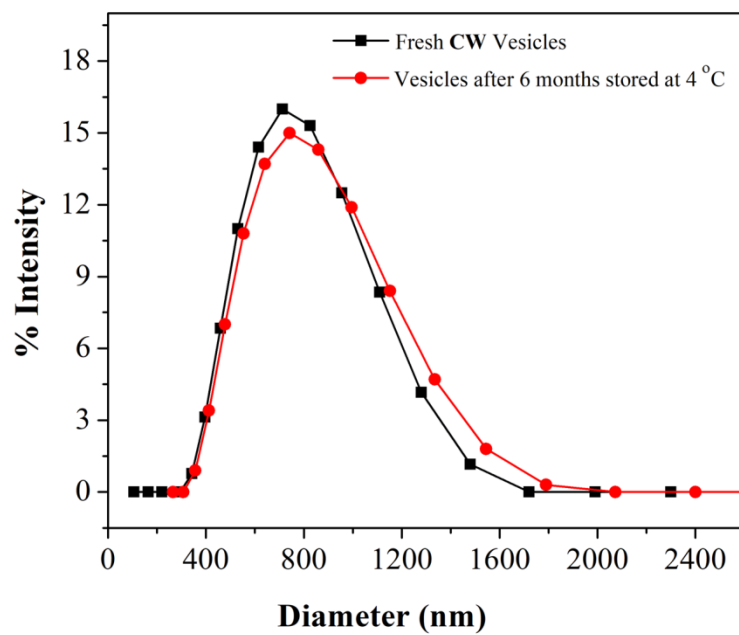


Figure S14: Aggregation study of empty CW vesicles stored at 4 °C using DLS data.

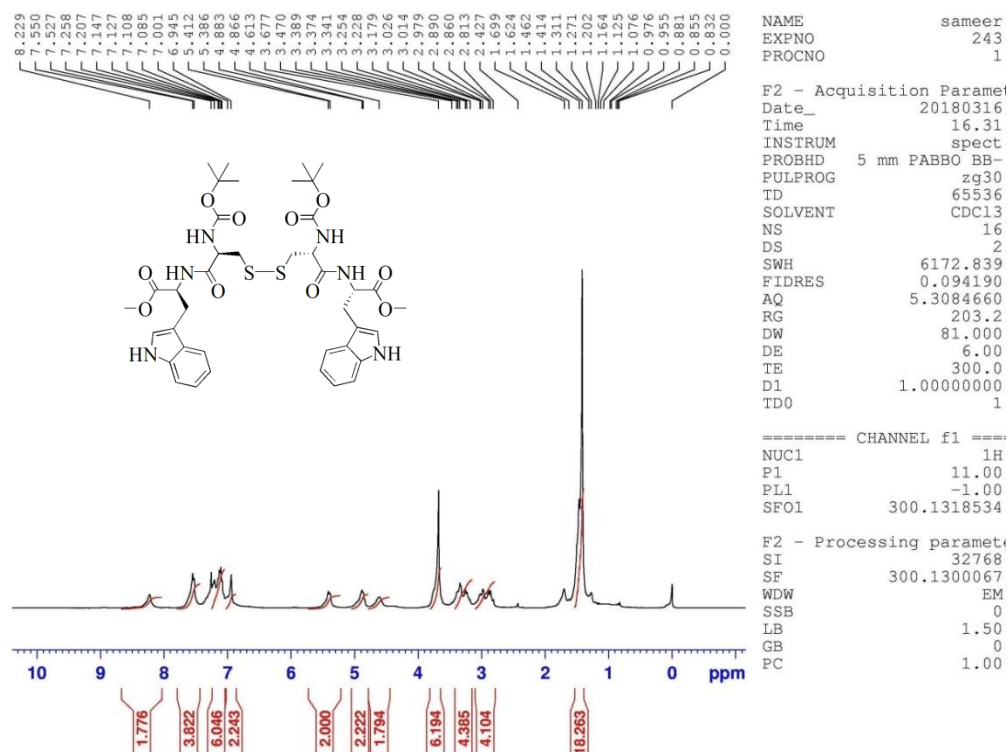


Figure S15: ^1H NMR spectrum (CDCl_3 , 300 MHz) of tryptophan-based dipeptide **BCW**.

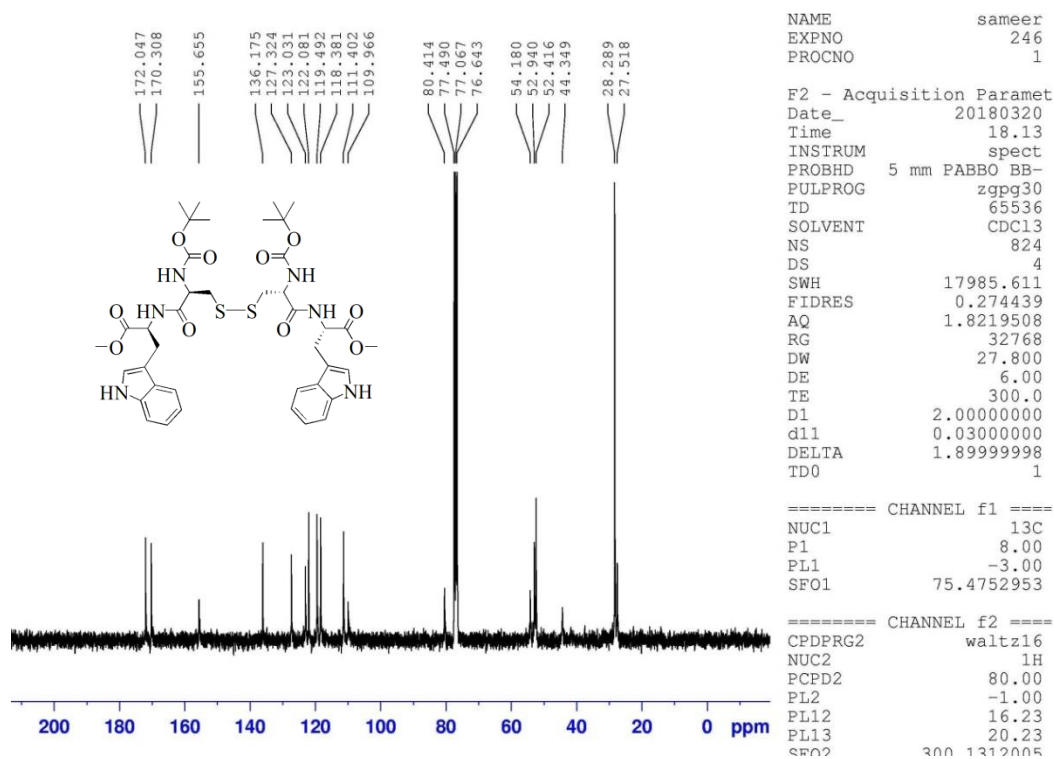


Figure S16: ^{13}C NMR spectrum (CDCl_3 , 75 MHz) of tryptophan-based dipeptide **BCW**.

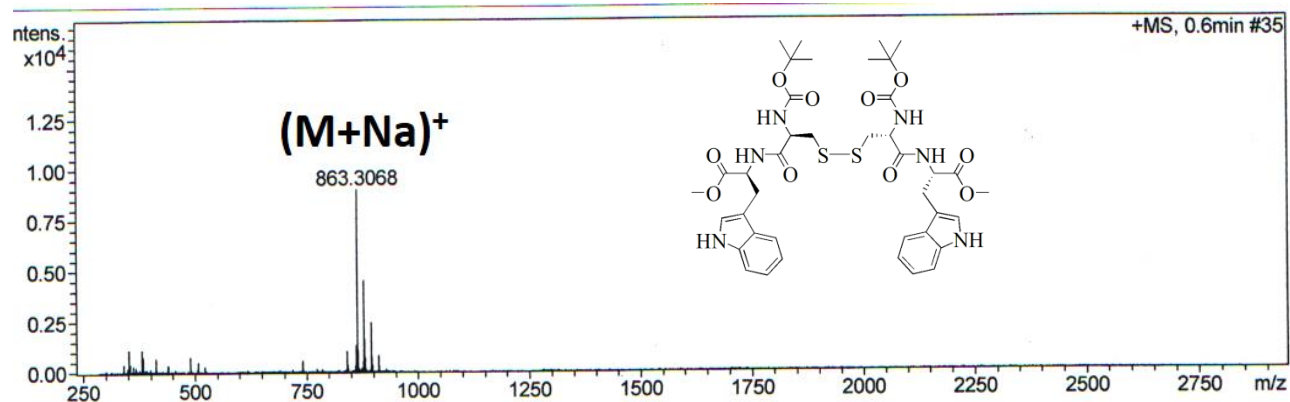


Figure S17: ESI-Mass spectrum of tryptophan-based dipeptide **BCW**.

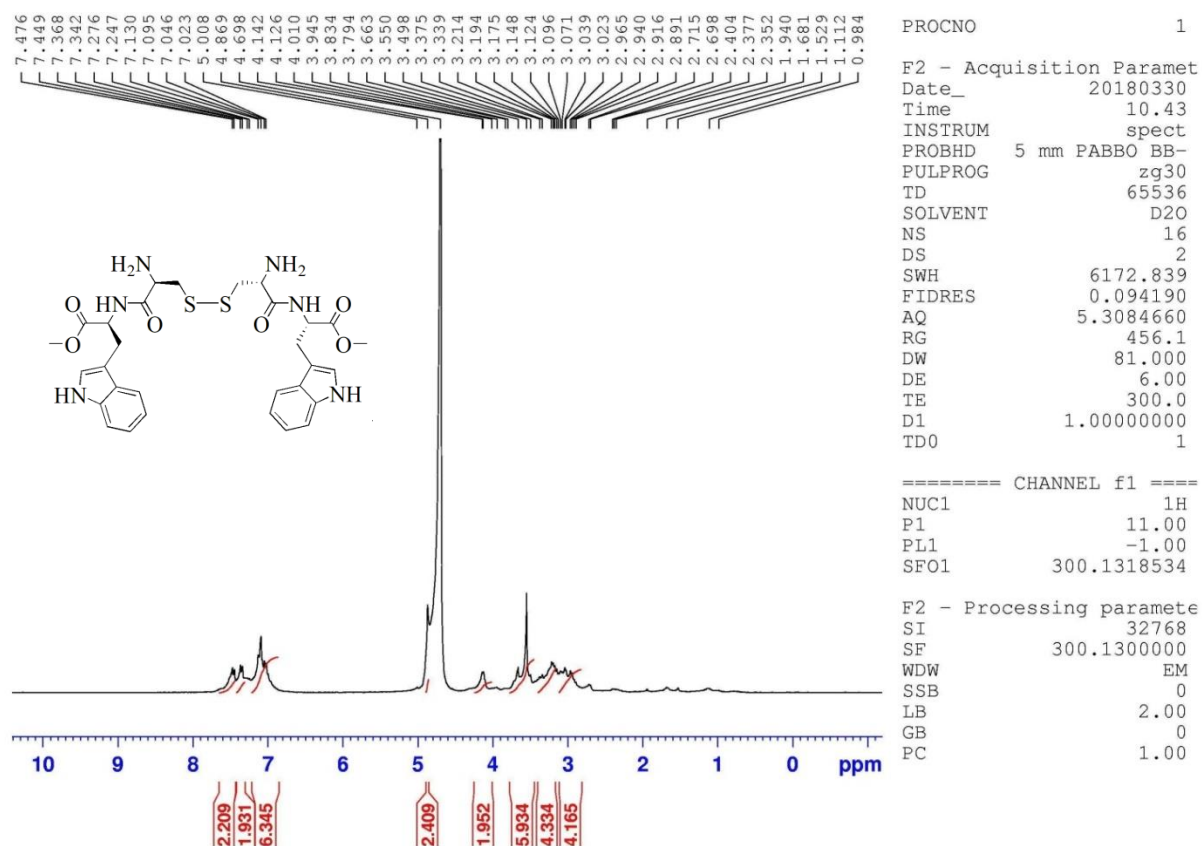


Figure S18: ^1H NMR spectrum (D_2O , 300 MHz) of diamine derivative **CW**.

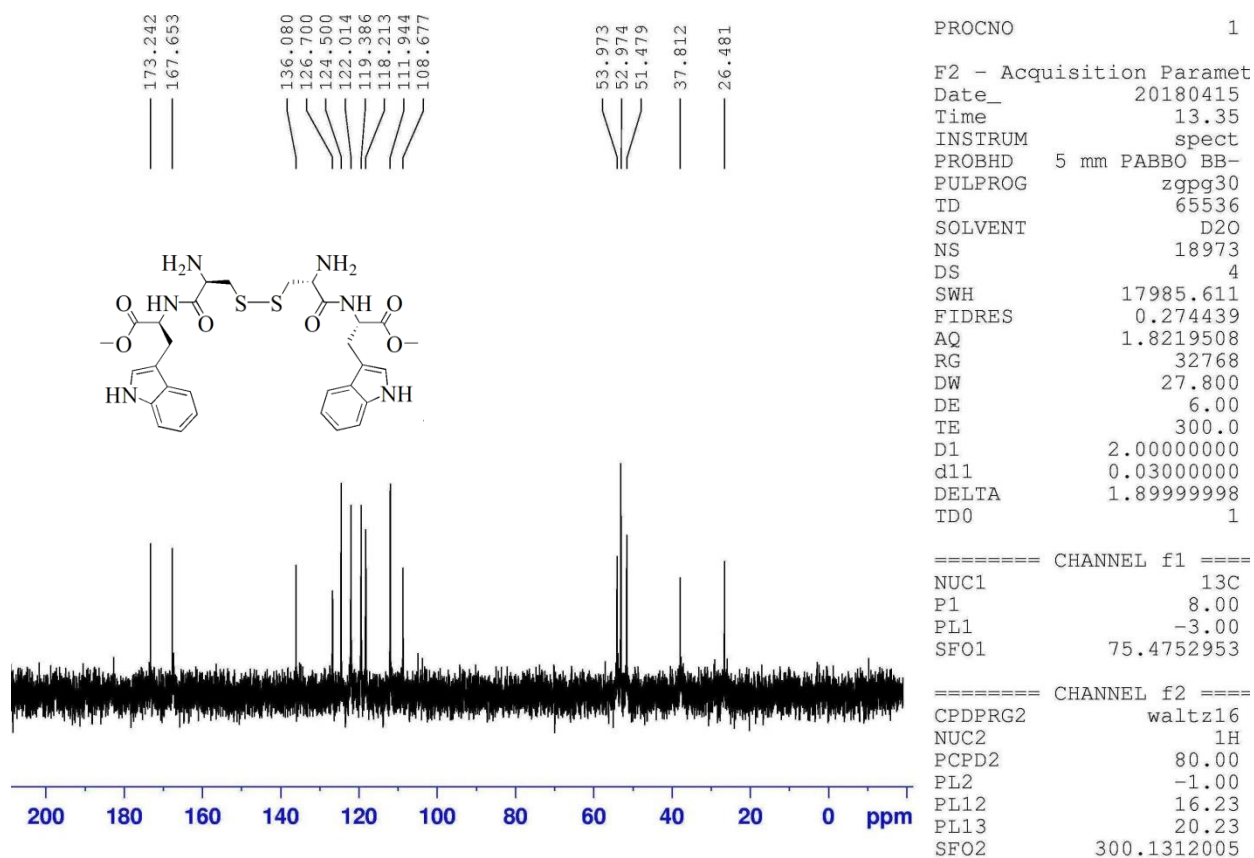


Figure S19: ¹³C NMR spectrum (D₂O, 75 MHz) of diamine derivative CW.

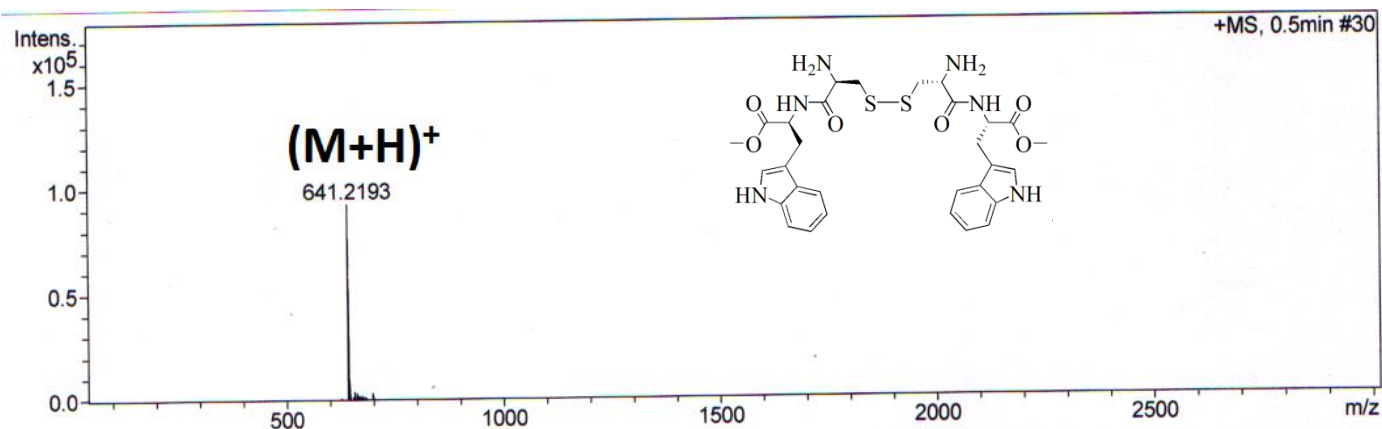


Figure S20: ESI-Mass spectrum of diamine derivative CW.

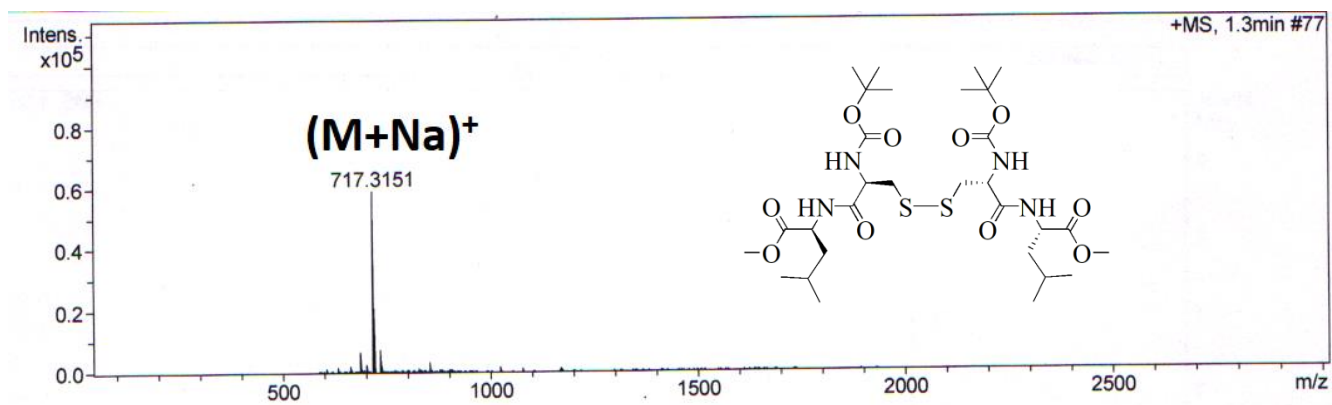


Figure S23: ESI-Mass spectrum of leucine-based dipeptide **3**.

References

- (1) Topel, Ö.; Çakır, B. A.; Budama, L.; Hoda, N. Determination of Critical Micelle Concentration of Polybutadiene-Block-Poly(ethyleneoxide) Diblock Copolymer by Fluorescence Spectroscopy and Dynamic Light Scattering. *J. Mol. Liq.* **2013**, *177*, 40–43. <https://doi.org/10.1016/j.molliq.2012.10.013>.
- (2) Humphrey, W.; Dalke, A.; Schulten, K. VMD: Visual Molecular Dynamics. *J. Mol. Graph.* **1996**, *14* (1), 33–38. [https://doi.org/10.1016/0263-7855\(96\)00018-5](https://doi.org/10.1016/0263-7855(96)00018-5).
- (3) Martínez, L.; Andrade, R.; Birgin, E. G.; Martínez, J. M. PACKMOL: A Package for Building Initial Configurations for Molecular Dynamics Simulations. *J. Comput. Chem.* **2009**, *30* (13), 2157–2164. <https://doi.org/10.1002/jcc.21224>.
- (4) Martínez, J. M.; Martínez, L. Packing Optimization for Automated Generation of Complex System's Initial Configurations for Molecular Dynamics and Docking. *J. Comput. Chem.* **2003**, *24* (7), 819–825. <https://doi.org/10.1002/jcc.10216>.
- (5) Phillips, J. C.; Braun, R.; Wang, W.; Gumbart, J.; Tajkhorshid, E.; Villa, E.; Chipot, C.; Skeel, R. D.; Kalé, L.; Schulten, K. Scalable Molecular Dynamics with NAMD. *J. Comput. Chem.* **2005**, *26* (16), 1781–1802. <https://doi.org/10.1002/jcc.20289>.
- (6) Brooks, B. R.; Brooks, C. L.; Mackerell, A. D.; Nilsson, L.; Petrella, R. J.; Roux, B.; Won, Y.; Archontis, G.; Bartels, C.; Boresch, S.; et al. CHARMM: The Biomolecular Simulation Program. *J. Comput. Chem.* **2009**, *30* (10), 1545–1614. <https://doi.org/10.1002/jcc.21287>.
- (7) Kumar, P. P. P.; Suresh, C. H.; Haridas, V. A Supramolecular Approach to Metal Ion Sensing: Cystine-Based Designer Systems for Cu²⁺, Hg²⁺, Cd²⁺ and Pb²⁺ Sensing. *RSC Adv* **2015**, *5* (11), 7842–7847. <https://doi.org/10.1039/C4RA14389B>.
- (8) Bai, T.; Du, J.; Chen, J.; Duan, X.; Zhuang, Q.; Chen, H.; Kong, J. Reduction-Responsive Dithiomaleimide-Based Polymeric Micelles for Controlled Anti-Cancer Drug Delivery and Bioimaging. *Polym. Chem.* **2017**, *8* (46), 7160–7168. <https://doi.org/10.1039/C7PY01675A>.